

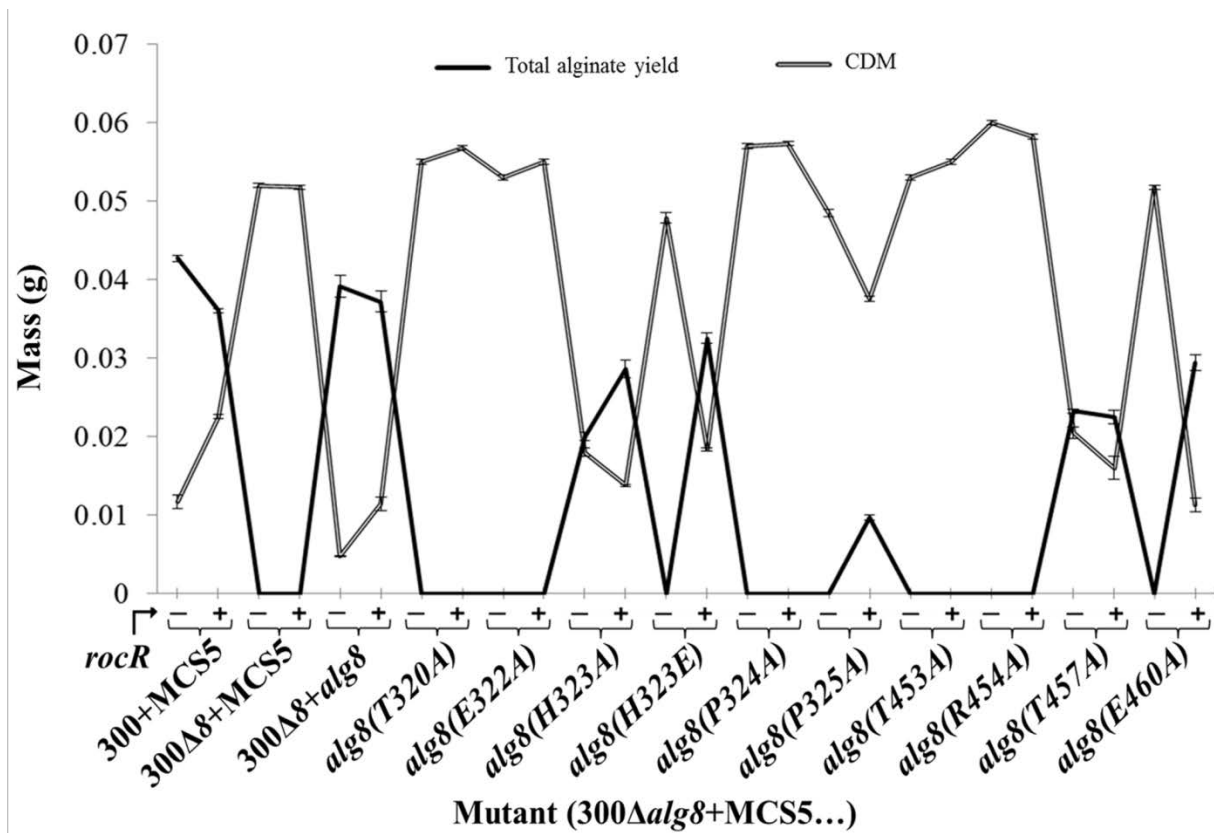
# Supplemental Materials

## **Activation Mechanism and Cellular Localization of Membrane-Anchored Alginate Polymerase in *Pseudomonas aeruginosa***

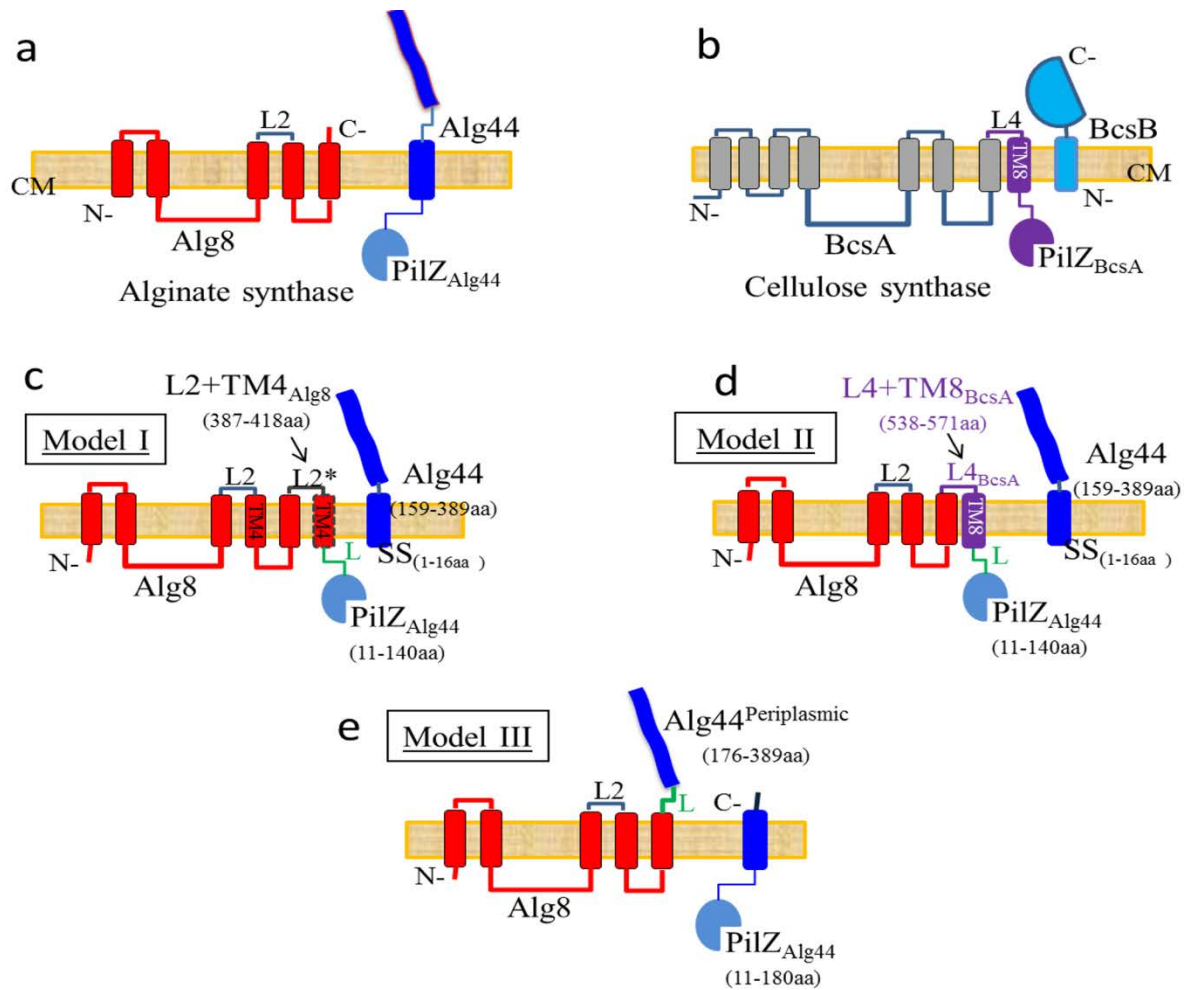
M. Fata Moradali, Shirin Ghods, Bernd H. A. Rehm <sup>a</sup>

Institute of Fundamental Sciences, Massey University, Private Bag 11222, Palmerston North, New Zealand

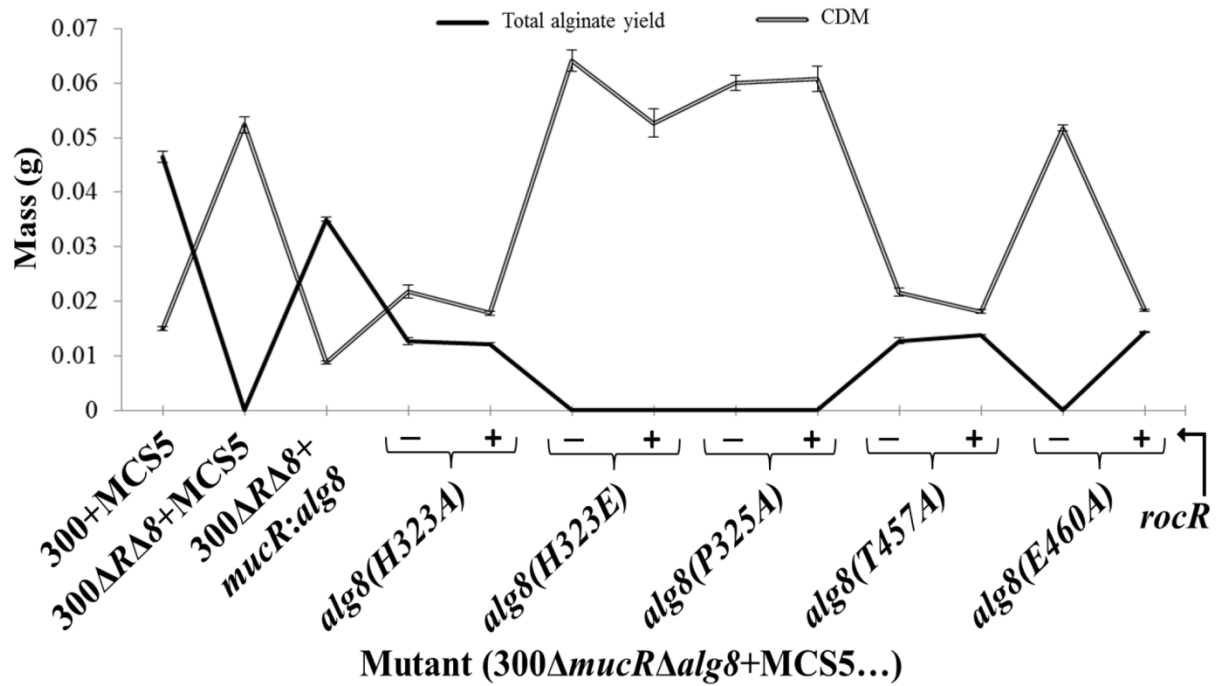




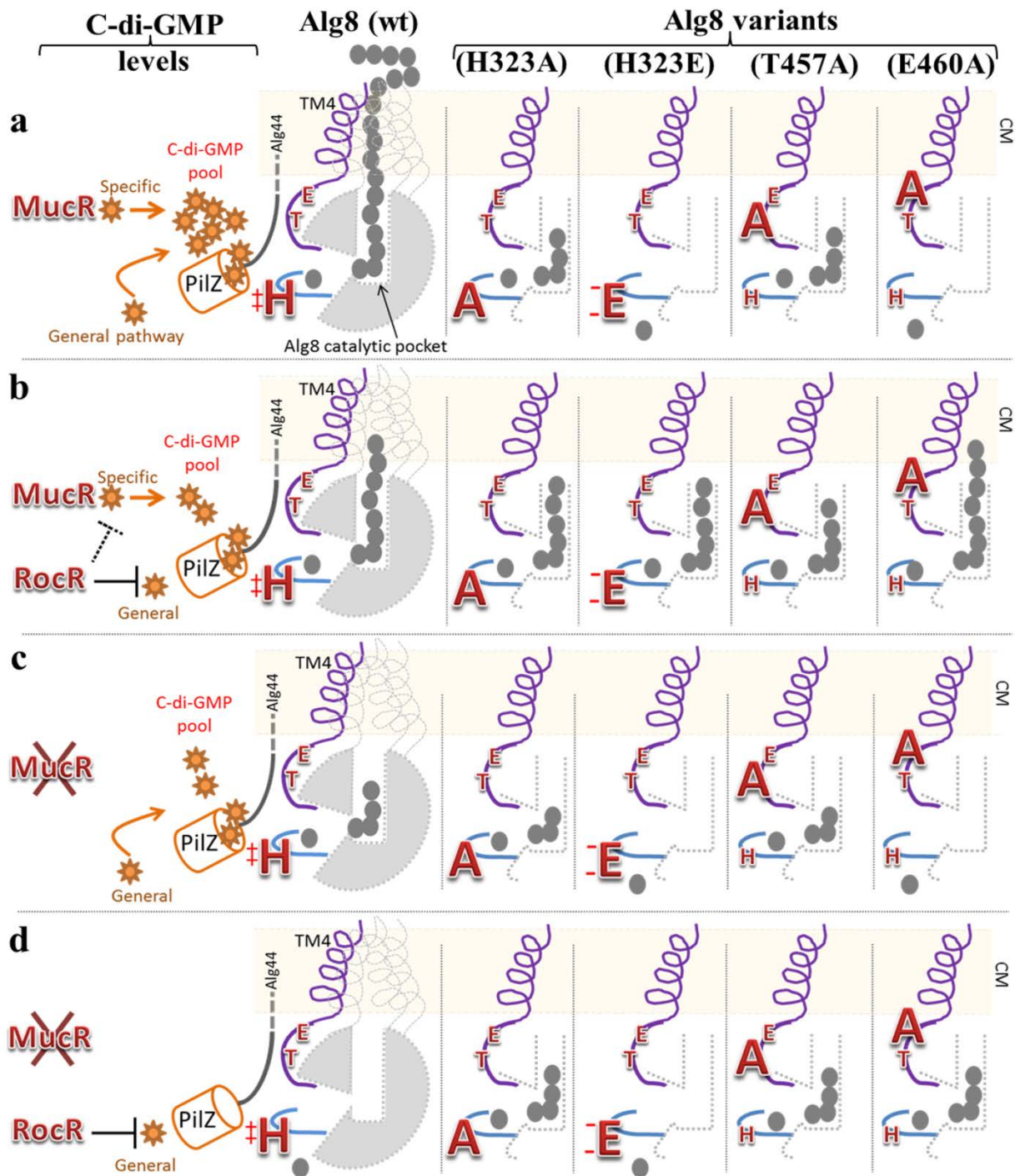
**Supplementary Figure S2. Correlation of dry cell mass (CDM) and total alginate yield produced by PDO300Δalg8 transformants harboring various plasmids containing respective site-specific mutagenesis variants of *alg8* with (+) and without (-) the *rocR* gene.** These quantifications are based on incubation of cells at 37 °C for 72 h grown on PIA medium (solid culture) containing 300 μg/ml of gentamicin. Data are means plus standard deviations of four independent repetitions. 300, PDO300; MCS5, pBBR1MCS-5.



**Supplementary Figure S3. Schematic fusion models of Alg8-Alg44-PilZ<sub>Alg44</sub> and BcsA were analyzed *in vivo*.** (a) Model of alginate synthase complex consisting of Alg8-Alg44 and (b) cellulose synthase complex including BcsA-BcsB proteins. One of the major structural differences between two complexes lies on the position of c-di-GMP sensing domain i.e. PilZ domain and the number and orientation of transmembrane domains. The C-terminal part of BcsA contains a transmembrane domain (TM) which extends into the cytoplasm leading to the PilZ domain while the C-terminal part of Alg8 is exposed to the periplasm and the PilZ domain is located at the N-terminal part of Alg44 in the cytoplasm. (c) the C-terminal fusion of Alg8 with a similar sequence of loop 2 (L2<sub>Alg8</sub>, labeled with star) and TM4<sub>Alg8</sub> was linked to PilZ<sub>Alg44</sub> domain via a five glycine linker (L). This was in combination with Alg44 without the N-terminal PilZ domain, but with signal sequence for localization into the cytoplasmic membrane. (d) the C-terminal fusion of Alg8 with a homologous sequence of L4<sub>BcsA</sub> and TM8<sub>BcsA</sub> was linked to PilZ<sub>Alg44</sub> domain via similar linker. This was in combination with Alg44 without the N-terminal PilZ domain, but with signal sequence for localization. (e) the C-terminal fusion of Alg8 was linked to the periplasmic domain of Alg44 via similar linker while it was combined with Alg44 without periplasmic domain. N-: N-terminal; C-: C-terminal; L2: loop 2; L4: loop 4; L: linker; aa: amino acid; SS: signal sequence; TM: transmembrane domain; CM: cytoplasmic membrane.

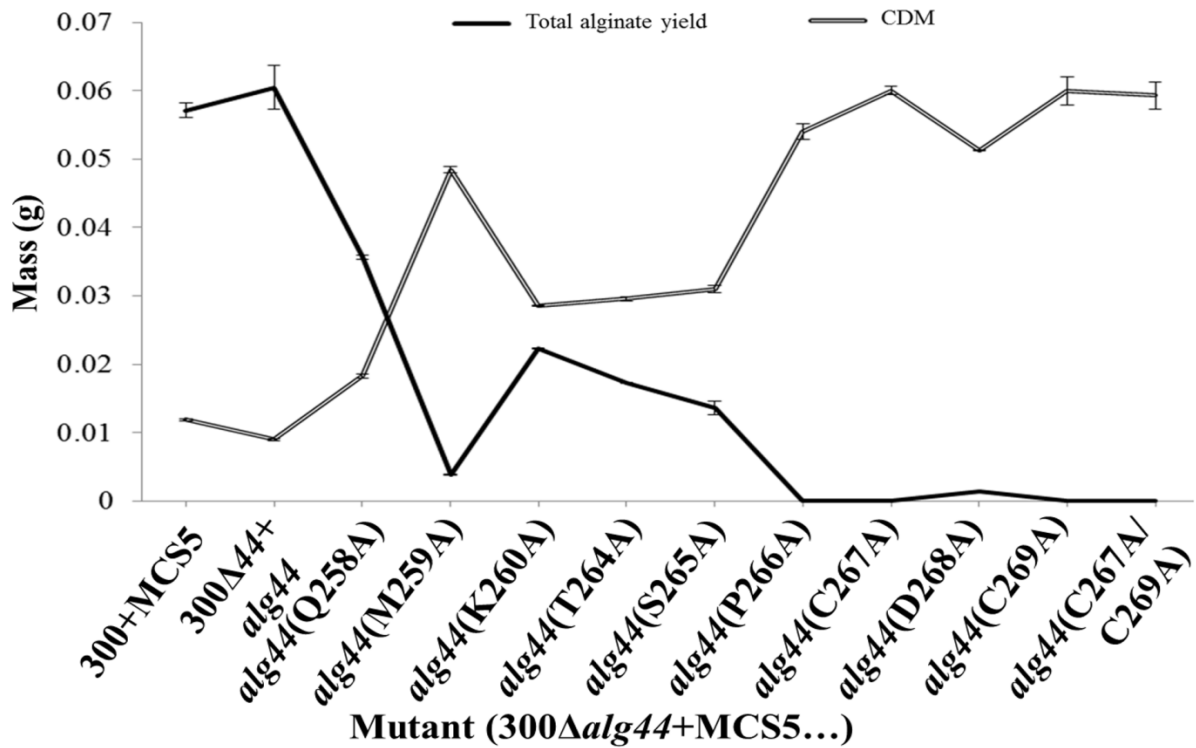


**Supplementary Figure S4. Correlation of dry cell mass (CDM) and total alginate yield produced by PDO300Δ*mucR*Δ*alg8* transformants harboring various plasmids containing respective site-specific mutagenesis variants of *alg8* with (+) and without (-) the *rocR* gene.** These quantifications are based on incubation of cells at 37 °C for 72 h grown on PIA medium (solid culture) containing 300 μg/ml of gentamicin. Data are means plus standard deviations of four independent repetitions. 300, PDO300; MCS5, pBBR1MCS-5.

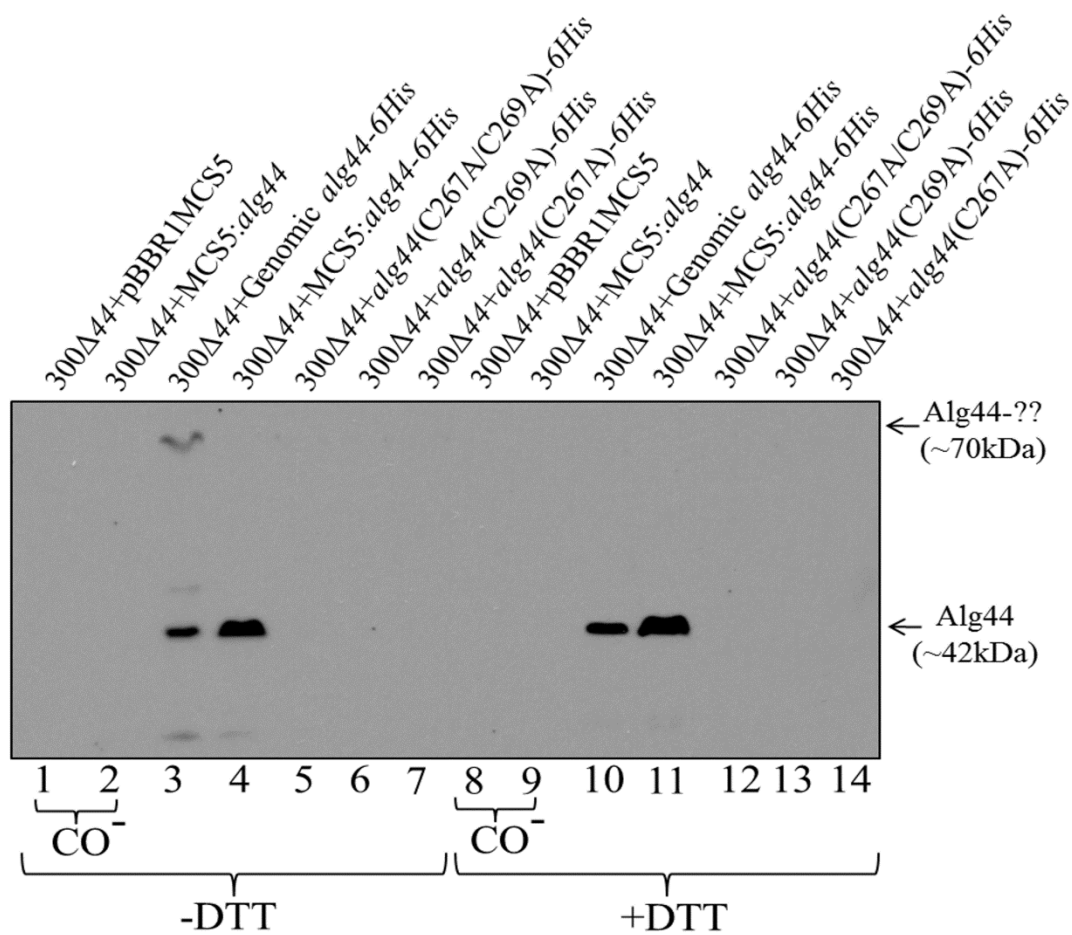


**Supplementary Figure S5. Proposed schematic representation of mutual and combinational effects of point-mutation of Alg8 residues including H323, T457 and E460 (red letters in wild-type (wt) column) and c-di-GMP levels (orange stars) (impacted by RocR and/or MucR) on activation of alginate polymerization.** Alginate synthesis is positively regulated by elevated levels of c-di-GMP in the cytosol (RocR degrades c-di-GMP in the cytosol) or specifically by MucR proposed to generate a localized pool of c-di-GMP in proximity to PilZ<sub>Alg44</sub>. Informed by the *in silico* model of Alg8-PilZ<sub>Alg44</sub>, three residues including H323 (on loop A), T457 and E460 (on loop B) were proposed as critical for c-di-GMP dependent activation of Alg8. The various levels of c-di-GMP and their impact on activation of alginate polymerization based on Alg8 variants were illustrated in rows **a-d** (enlarged bold letters

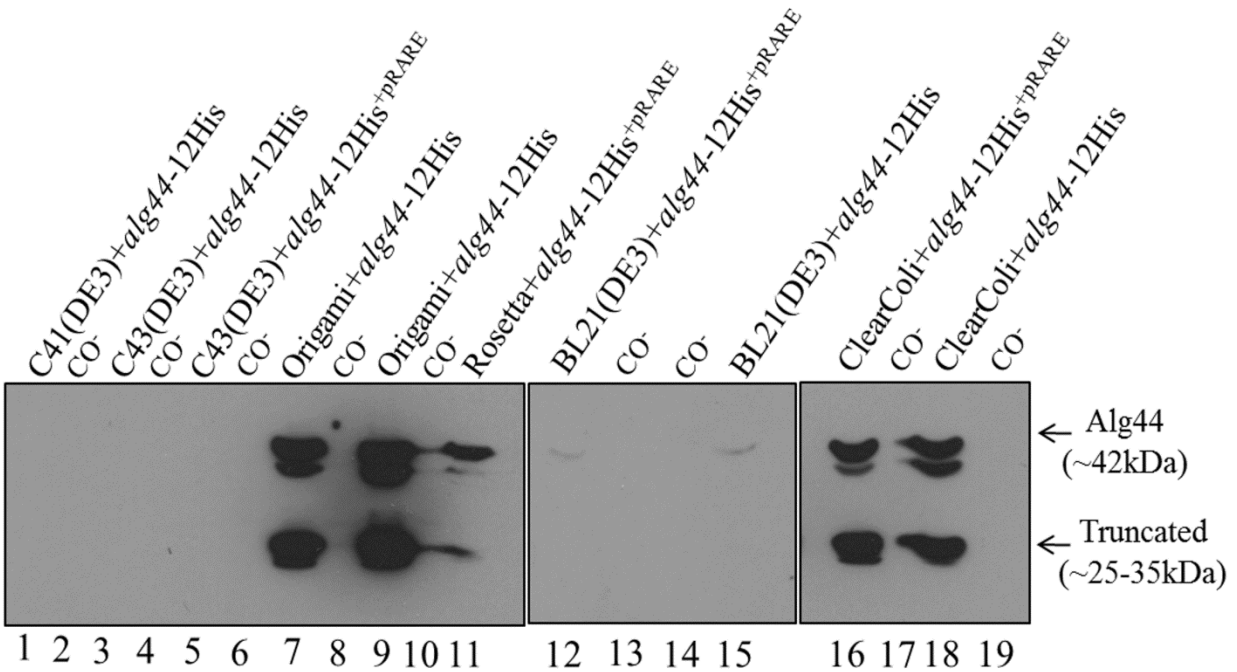
represent replaced residues). Remarkably, high c-di-GMP levels caused inhibition in H323E and E460A variants (row **a**), while RocR mediated reduction of c-di-GMP levels mediated activation of alginate polymerization (row **b**). The H323E variant was not active in the MucR knockout mutant (row **c** and **d**), while H323A, T457A and E460A variants retained functionality independent from c-di-GMP depletion due to the absence of MucR and the presence of RocR overproduction (row **d**). Gray circles represent monomeric units (mannuronic acid); TM4, transmembrane domain 4; CM, cytoplasmic membrane.



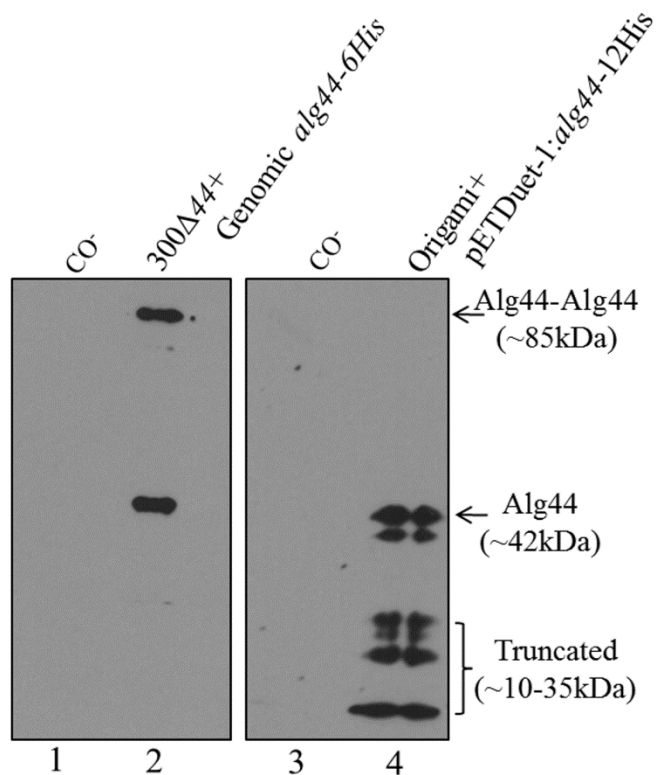
**Supplementary Figure S6. Correlation of dry cell mass (CDM) and total alginate yield produced by PDO300Δ*alg44* transformants harboring various plasmids containing respective site-specific mutagenesis variants of *alg44* gene.** These quantifications are based on incubation of cells at 37 °C for 72 h grown on PIA medium (solid culture) containing 300 μg/ml of gentamicin. Data are means plus standard deviations of four independent repetitions. 300, PDO300; MCS5, pBBR1MCS-5.



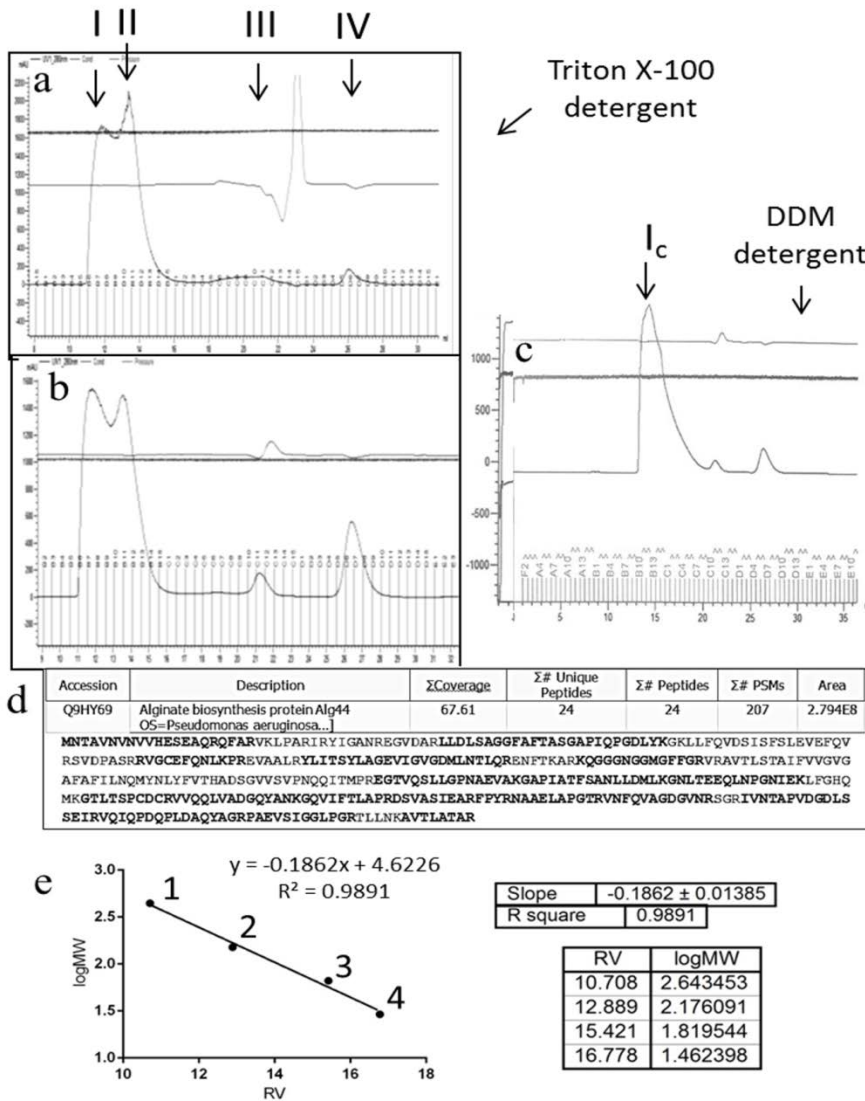
**Supplementary Figure S7. Disulfide bond formation in Alg44 and impact on dimerization/protein-protein interactions.** Immunoblot analysis of envelope fractions developed using anti-His-tag antibodies showed that a protein band with greater apparent molecular weight (~70 kDa) was detected without DTT treatment (lane 3) while it was missing after addition of DTT (lane 10) or when protein was produced encoded from plasmid (lanes 4 and 11). Immunoblot analysis confirmed Alg44 is missing when cysteine residues were replaced with alanine (lanes 5-7 and 12-14). Lanes 1-2 and 8-9 represent negative controls. 300: PDO300; MCS5: pBBR1MCS-5; Co<sup>-</sup>: negative control.



**Supplementary Figure S8. Assessment of heterologous production of Alg44 using immunoblotting and anti-His-tag antibodies.** In order to analyze the quaternary structure of Alg44 and to assess the heterologous production of this protein for purification and *in vitro* functional/structural analyses, we screened different strains of *E. coli* for the expression of the full length *alg44-12His* gene. Briefly, strains C41(DE3) and C43(DE3) (lanes 1, 3, and 5) did not show any detectable protein production and BL21(DE3) (lanes 12 and 15) showed only weak production while Origami™ (DE3) (lanes 7 and 9), ClearColi BL21(DE3) (lanes 16 and 18) and Rosetta™ strains (lane 11) gave rise to higher protein production levels of the *alg44-12His* gene when compared with the other strains (Fig. S5). However, a significant fraction of protein was subjected to proteolytic truncation during membrane isolation even in the presence of protease inhibitors (Fig. S5). However, in all cases recombinant Alg44 was truncated. All genes were inserted into pETDuet-1 vector. Negative controls harbored empty plasmids. Co<sup>-</sup>: negative control.

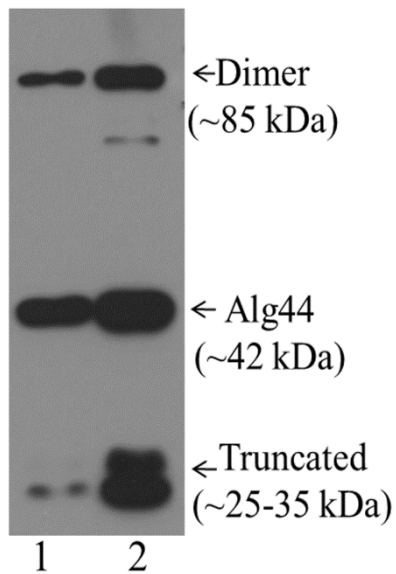


**Supplementary Figure S9. His-affinity chromatography purification of Alg44 produced by homologous *P. aeruginosa* (left) and heterologous *E. coli* (right) hosts.** Immunoblot analysis using anti-His-tag antibodies showed when EDTA was added, the presence of two distinct bands corresponding to the molecular weight of Alg44 monomer and dimer (lane 2) while heterologous Alg44 was truncated (lane 4). Negative controls harbored empty plasmids. 300: PDO300; MCS5: Co<sup>-</sup>: negative control i.e. *P. aeruginosa* PDO300 or *E. coli* Origami (pETDuet-1).

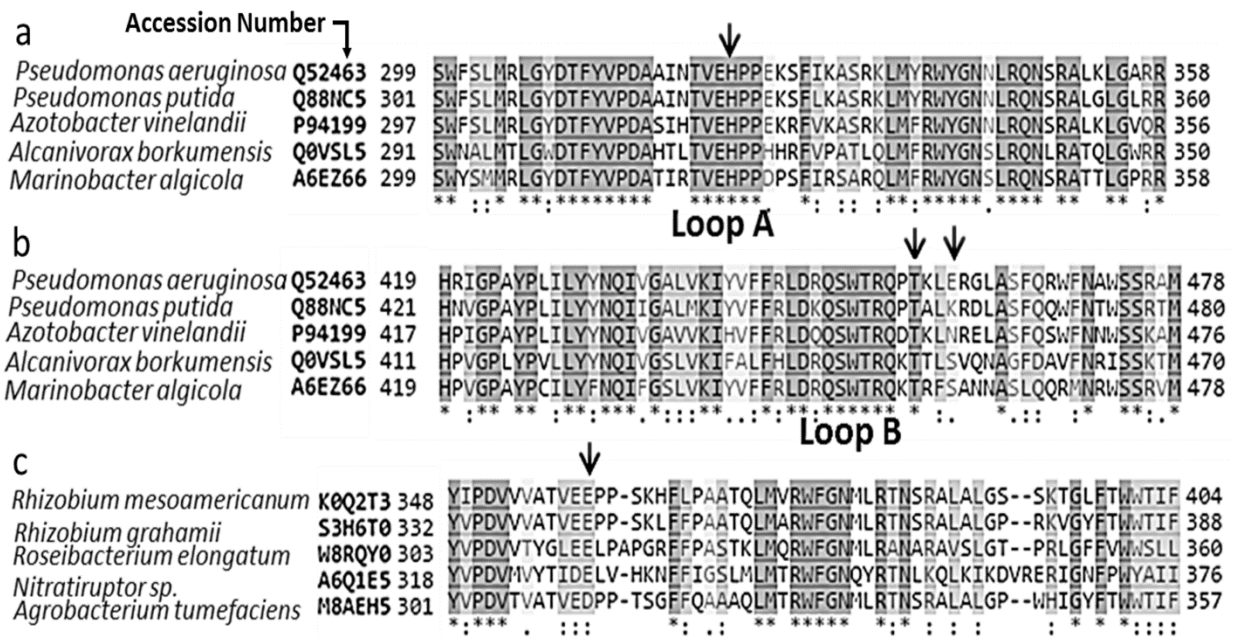


**Supplementary Figure S10. Gel filtration chromatogram showing purification of the Alg44 dimer.** (a-b) Chromatograms belong to purification of Alg44-6His from a partially purified sample (provided using His-tag affinity chromatography), before (a) and after (b) treatment with triton X-100, alginate solution and DTT. Two major peaks I and II were separated in panels a and b. Presumable impurities associated with these peaks were removed after treatment of protein sample with 0.2% (wt/vol) alginate solution and 50 mM DTT and resulted in peaks III and IV appearance (b). Protein analysis using immunoblotting showed peak I which was collected in three 500- $\mu$ L fractions (at  $K_{av}$ : 11-13) containing oligomeric states of Alg44 which was detected as Alg44 dimer under denaturing condition using SDS-PAGE and immunoblotting. Protein concentration in each fraction of peak I was quantified as 2.88-2.99 mg/mL. Peak II was not detectable and identifiable using SDS-PAGE or immunoblotting. (c) replacement of triton X-100 by DDM resulted in resolving one peak corresponding to an apparent MW of 83.7 kDa indicating the presence of the Alg44 dimer. Similarly a band corresponding to stable Alg44 dimer was detected by immunoblotting. (d) Protein sequence of the purified protein showed the

existence of Alg44 with its signal peptide. Bold letters indicate identified peptides by mass spectrometry. (e) Molecular weight standard curve was applied to calculate protein molecular weights (for detail of calculation see materials and methods).



**Supplementary Figure S11.** Immunoblot analysis (lanes 1 and 2) showed that treatment of the sample with n-Dodecyl  $\beta$ -D-maltoside (DDM) during purification of Alg44 resulted in reduction of Alg44 dimer stability and more truncations. Immunoblots were developed using anti-His-tag antibodies.



**Supplementary Figure S12. Loops A and B of Alg8 are highly conserved among alginate-producing bacteria and others with Alg8 homologous counterparts.** Multiple alignments of loop A (a) and loop B (b) among Gamma-proteobacteria which produce alginate show highly conserved sequences. Arrows show respectively H323 (a), T457 and E460 (b) of *P. aeruginosa* which are respectively highly and less conserved, but their mutations identified with the most significant effect on regulation of alginate production. (c) Multiple alignments of the loops homologues to loop A of Alg8, but originating from Alpha-proteobacteria and Epsilon-proteobacteria show H323 of Alg8 is replaced with a negatively charged amino acid.

**Supplementary Table S1.** Composition of alginates produced by different variants of Alg44

Mutants	Ac%	$F_M$	$F_G$	$F_{MG/GM}$	$F_{MM}$
300+MCS5	52	0.6	0.4	0.4	0.2
$\Delta 44+44his$	64	0.86	0.14	0.14	0.72
Q258A	50	0.8	0.2	0.2	0.6
M259A	38	0.7	0.3	0.3	0.4
K260A	49	0.8	0.2	0.2	0.6
T264A	52	0.78	0.22	0.22	0.56
S265A	49	0.86	0.14	0.14	0.72
D268A	34	0.77	0.23	0.23	0.54

300:PDO300; MCS5: pBBR1MCS-5;  $F_G$ : molar fraction of guluronate (G) residue;  $F_M$ : molar fraction of mannuronate (M) residue;  $F_{GM/MG}$ : molar fraction of two consecutive G and M residues;  $F_{MM}$ : molar fraction of two consecutive M residues; Ac.: acetylation

**Supplementary Table S2.** Composition of alginates produced by various *Paeruginosa* strains and impacted by Alg44 variants (values arranged in descending order)

Mutant	$F_G$	Mutant	Ac%	Mutant	$F_{MM}$
300+MCS5	0.4	$\Delta 44+44his$	64	$\Delta 44+44his$	0.72
M259A	0.3			S265A	0.72
D268A	0.23	300+MCS5	52	Q258A	0.6
T264A	0.22	T264A	52	K260A	0.6
Q258A	0.2	Q258A	50	T264A	0.56
K260A	0.2	K260A	49	D268A	0.54
		S265A	49		
$\Delta 44+44his$	0.14	M259A	38	M259A	0.4
S265A	0.14	D268A	34	300+MCS5	0.2

300:PDO300; MCS5: pBBR1MCS-5;  $F_G$ : molar fraction of guluronate (G) residue;  $F_{MM}$ : molar fraction of two consecutive M residues; Ac.: acetylation